High-Field Superconductivity of Carbides*

H. J. FINK AND A. C. THORSEN†
Atomics International Division of North American Aviation, Inc., Canoga Park, California

AND

EARL PARKER, VICTOR F. ZACKAY, AND LOU TOTH‡
Inorganic Materials Research Division, Lawrence Radiation Laboratory and Department of Mineral Technology, College of Engineering, University of California, Berkeley, California

(Received 21 December 1964)

The high-magnetic-field properties of some refractory carbides were investigated at low temperatures. The upper critical fields for NbC, a solid solution of 40% NbC-60% TaC, and TaC are between 4.2 and 21.3 kG; MoC, $Mo_{56}C_{44}$, and $Mo_{60}C_{40}$+2% VC have upper critical fields between 80 and 120 kG; and Mo_3Al_2C has an upper critical field of 156 kG at 1.2°K. Mo_3Al_2C is the only known superconductor with the β-Mn crystal structure. From the available data the electronic specific-heat coefficient γ, the thermodynamic critical field H_c, the Ginzburg-Landau parameter κ, and the lower critical field H_{c1} were estimated at the experimental temperatures.

INTRODUCTION

SYSTEMATIC studies of the carbides have shown that some of the investigated materials have transition temperatures in the neighborhood of 10°K and high normal-state resistivities. These facts lead one to suspect that some of these materials might be high-field superconductors. We have investigated the resistive transitions at constant current in high magnetic fields for NbC, a solid solution of 40% NbC–60% TaC, TaC, MoC, $Mo_{56}C_{44}$, $Mo_{60}C_{40}$+2% VC, and Mo_3Al_2C. From the upper critical field, the normal-state resistivity, and the transition temperature, we have evaluated the electronic heat coefficient γ, the thermodynamic critical field H_c, the lower critical field H_{c1}, and the Ginzburg-Landau parameter κ.

EXPERIMENTAL PROCEDURES AND RESULTS

The preparation of these materials has been described elsewhere.[1–3] The resistive transitions from the superconducting to the normal state were measured

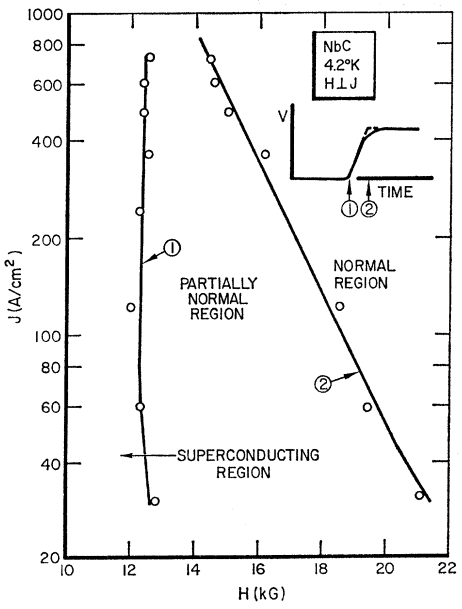

FIG. 1. The current densities as a function of magnetic field for NbC at the superconducting-partially normal boundary and at the partially normal-normal boundary. The temperature was 4.2°K and the applied magnetic field was perpendicular to the current.

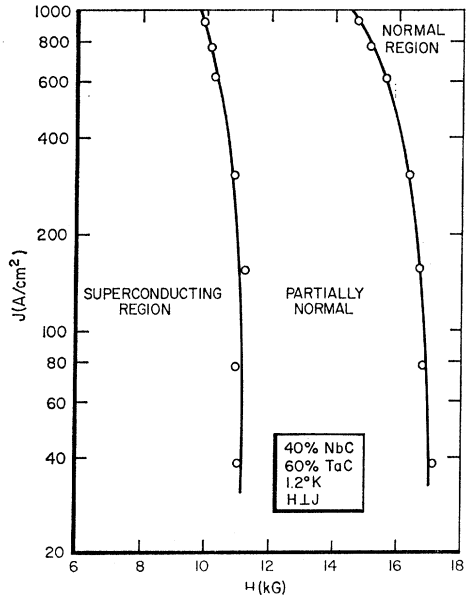

FIG. 2. The current densities as a function of magnetic field for 40% NbC–60% TaC at the superconducting-partially normal boundary and at the partially normal-normal boundary. The temperature was 1.2°K and the applied magnetic field was perpendicular to the current.

* Supported by the U. S. Atomic Energy Commission.

† Present address: North American Aviation Science Center, Thousand Oaks, California.

‡ Present address: Materials Science Department, University of Minnesota, Minneapolis, Minnesota.

[1] J. Johnston, L. Toth, K. Kennedy, and E. R. Parker, Solid State Commun. 2, 123 (1964).

[2] M. Wells, M. Pickus, K. Kennedy, and V. Zackay, Phys. Rev. Letters 12, 536 (1964).

[3] L. E. Toth, V. F. Zackay, J. Johnston, M. Wells, and E. R. Parker, Acta Met. (to be published).

TABLE I. Material investigated; crystal structure; cross-sectional area A of the samples; transition temperature in zero magnetic field T_c; the temperature at which the experiment was performed T_{exp}; the range of magnetic fields over which the material goes from the superconducting to the normal state for the smallest current densities used in these experiments (see Figs. 1 to 6); and normal state resistivity ρ_n.

Material	Crystal structure	$A\times10^3$ (cm²)	T_c (°K)	T_{exp} (°K)	$(H_s; H_n)$ (kG)	ρ_n ($\mu\Omega$-cm)
NbC	all cubic	8.28	8 –10[3]	4.2	12.6; 21.3	35.1
40% NbC–60% TaC	all cubic	6.59	10 –13.6[2]	1.2	11.2; 17.0	30.7
TaC	all cubic	7.69	9 –11.4[2]	1.2	4.2; 5.0[c]	12.7
MoC	cubic[a] plus hex.	7.27	12.5–13.5[3]	1.2	95; 120	26.6
$Mo_{56}C_{44}$	mostly cubic but containing hex. phase	2.04	12.5–13.5[3]	1.2	87; 110	128
$Mo_{60}C_{40}$+2% VC	mostly single phase	2.57	11.2–13.2[3]	1.2	80; 120	9.93
Mo_3Al_2C	mostly β-Mn[b], trace secondary phase	3.31	9.8–10.2[1]	1.2	155; 157	98.7

[a] The equilibrium phase is hexagonal at room temperature. This sample was quenched from above 2200°C which "freezes in" the cubic phase. The latter is stable above 2200°C but metastable at low temperatures.
[b] 54 ions per "cubic unit cell."
[c] At $J=65$ A/cm².

in high-pulsed magnetic fields at various current densities and at constant temperature. The experimental method is similar to that employed by Berlincourt and Hake.[4] The "spark-cut" samples were 1.0 to 1.2 cm long with the ends copper-plated and soldered to the current leads. The voltage terminals were applied by pressure to the samples and the distance between them ranged from 0.2 to 0.4 cm. The cross-sectional areas A of the samples are shown in Table I. The pulsed magnetic fields were applied perpendicular to the current flow through the samples. The transition temperatures of the samples were measured previously,[1–3] and are not sharply defined (see Table I). The ranges of the magnetic fields over which the material goes from the superconducting (H_s) to the normal state (H_n) for the smallest current densities used in this experiment, the normal-state resistivities ρ_n, and the experimental temperatures, are also given in Table I.

The critical-field curves for various current densities[5] for NbC, 40% NbC–60% TaC, MoC, $Mo_{56}C_{44}$, and $Mo_{60}C_{40}$+2% VC are shown in Figs. 1 through 5. The spread between the superconducting and normal regions shown in the figures is generally large. The width of the "partially normal" region may be due to inhomogeneities and the presence of other phases. For TaC, the transition from the superconducting to the normal state occurred between 4.2 and 5 kG at current densities of 65 A/cm².

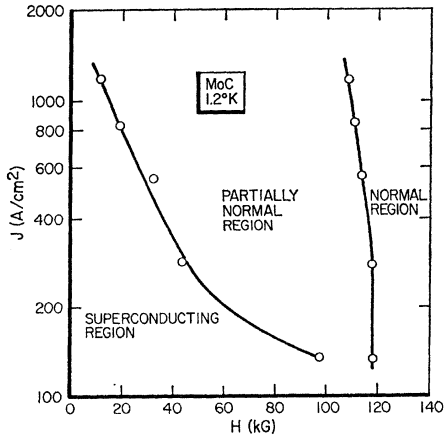

FIG. 3. The current densities as a function of magnetic field for MoC at the superconducting-partially normal boundary and the partially normal-normal boundary. The temperature was 1.2°K and the applied magnetic field was perpendicular to the current.

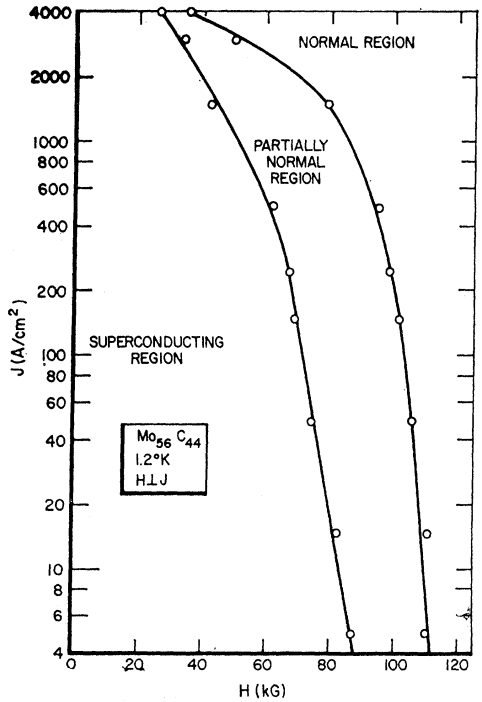

FIG. 4. The current densities as a function of magnetic field for $Mo_{56}C_{44}$ at the superconducting-partially normal boundary and at the partially normal-normal boundary. The temperature was 1.2°K and the applied magnetic field was perpendicular to the current.

[4] T. G. Berlincourt and R. R. Hake, Phys. Rev. 131, 140 (1963).

[5] The current density was calculated by dividing the current by the cross-sectional area. Since some of the samples were porous or inhomogeneous, the actual current densities were probably higher.

Figure 6 shows for Mo_3Al_2C the current density as a function of the applied magnetic field transverse to the current. There are again three distinct regions: the superconducting region where the resistance is zero; the normal region where the resistance is a constant; and a region in which the resistance is partially restored. Also, a sharp superconducting peak is observed at large magnetic fields. A hint of such a "peak effect" was first observed by Berlincourt[6] as an anomaly in the resistance as a function of magnetic field. Le Blanc and Little[7] then found an anomaly in the critical current as a function of magnetic field. Later Berlincourt, Hake, and Leslie[8] showed that the above two observations were simply different manifestations of the same "peak effect." The authors know of no satisfactory theory which explains this "peak effect." The inserts on the right of Fig. 6 show schematically the observed magnetic field and the voltage across the potential leads on the sample as a function of time. When the Mo_3Al_2C ribbon was rotated by 90° ($H_\perp$ was perpendicular to the current and also perpendicular to the broad face of the ribbon) essentially the same results were obtained as in Fig. 6. The ridge and the valley meet at a value of the resistance of about 0.63 of the normal-state resistance.

ESTIMATION OF PHYSICAL PARAMETERS

From the experimentally determined values of the upper critical field H_{c2}, transition temperature T_c, and normal state resistivity ρ_n, it is possible to derive approximate values of some of the other physical parameters of these materials. In particular, the electronic specific-heat coefficient γ, the thermodynamic critical field H_c, the lower critical field H_{c1}, and the Ginzburg-Landau parameter κ can be estimated using the formalism of the Bardeen-Cooper-Schrieffer and Ginzburg-Landau-Abrikosov-Gor'kov theories. Let us make use of the Bardeen-Cooper-Schrieffer[9] relation

$$\gamma T_c^2 \approx 0.17 H_0^2, \tag{1}$$

the thermodynamic critical field relation

$$H_c \approx H_0[1-(T/T_c)^2], \tag{2}$$

and the Ginzburg-Landau parameter[10–12]

$$\kappa = \kappa_0 + \kappa_l = \kappa_0 + C\rho_n\gamma^{1/2}, \tag{3}$$

where H_0 is the thermodynamic critical field at absolute zero, $\kappa=\lambda/\xi$, λ is the penetration depth, ξ is the coherence length and C is a constant $=7.55\times10^{-6}$ emu. κ can be represented as the sum of two limiting forms, namely κ_0 and κ_l. For κ_0 the coherence length is limited entirely by the electronic properties of the Fermi surface of the particular metal, and for κ_l the coherence length is limited only by the electron mean free path due to scattering of the electrons by impurities and defects.

The upper critical field H_{c2} is[13,14]

$$H_{c2} = A(T)\kappa H_c, \tag{4}$$

where the temperature dependence[14] $A(T)=1.77-0.43(T/T_c)^2+0.07(T/T_c)^4$ is an approximation only, but for the present estimates the uncertainty in $A(T)$ is overlooked. When Eqs. (1) to (4) are combined and κ_0 is neglected with respect to κ_l, one obtains for the electronic specific heat coefficient γ per unit volume (in emu)

$$\gamma = 5.47\times10^4 \frac{H_{c2}}{A(T)\rho_n T_c[1-(T/T_c)^2]}. \tag{5}$$

It will be shown below that it is a fair approximation for most of our samples to neglect κ_0.

With an average transition temperature $\langle T_c\rangle$, we have calculated γ from Eq. (5) at the experimental temperature T_{exp}, and show these values in Table II. The upper critical field H_{c2} was calculated somewhat arbitrarily from the data in Table I according to H_{c2}

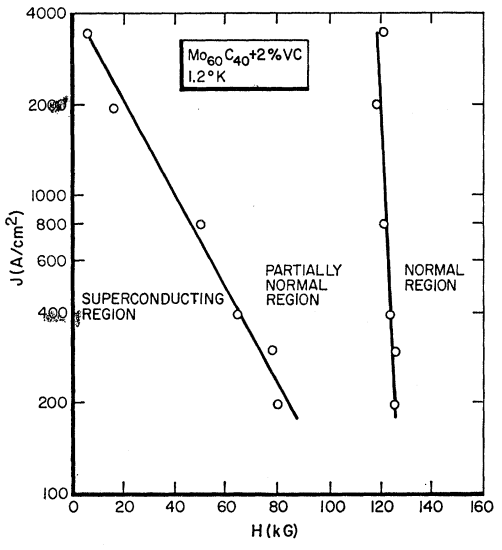

FIG. 5. The current densities as a function of magnetic field for $Mo_{60}C_{40}$+2% VC at the superconducting-partially normal boundary and at the partially normal-normal boundary. The temperature was 1.2°K and the applied magnetic field was perpendicular to the current.

[6] T. G. Berlincourt, Phys. Rev. **114**, 969 (1959).
[7] M. A. R. Le Blanc and W. A. Little, *Proceedings of the Seventh International Conference on Low Temperature Physics* (University of Toronto Press, Toronto, 1961), p. 362.
[8] T. G. Berlincourt, R. R. Hake, and D. H. Leslie, Phys. Rev. Letters **6**, 671 (1961).
[9] J. Bardeen, L. N. Cooper, and J. R. Schrieffer, Phys. Rev. **108**, 1175 (1957).
[10] V. L. Ginzburg and L. D. Landau, Zh. Eksperim. i Teor. Fiz. **20**, 1064 (1950).
[11] L. P. Gor'kov, Zh. Eksperim. i Teor. Fiz. **37**, 1407 (1959) [English transl.: Soviet Phys.—JETP **10**, 998 (1960)].
[12] B. B. Goodman, IBM J. Res. Develop. **6**, 63 (1962).
[13] A. A. Abrikosov, Zh. Eksperim. i Teor. Fiz. **32**, 1442 (1957) [English transl.: Soviet Phys.—JETP **5**, 1174 (1957)].
[14] L. P. Gor'kov, Zh. Eksperim. i Teor. Fiz. **37**, 835 (1959) [English transl.: Soviet Phys.—JETP **10**, 593 (1960)].

TABLE II. Material investigated; assumed average transition temperature $\langle T_c \rangle$; assumed upper critical field H_{c2} which was calculated from $\frac{1}{2}(H_s+H_n)$ at T_{exp}; electronic specific-heat coefficient γ; Ginzburg-Landau parameter κ_l at T_{exp} which arises from the scattering of the electrons only; the ratio of the estimated Ginzburg-Landau parameters due to the impurity scattering and that due to the electronic structure of the metal κ_l/κ_0 at T_{exp}; thermodynamical critical field H_c at T_{exp}; lower critical field H_{c1} at T_{exp}; the Clogston limit H_p at T_{exp}.

Material	$\langle T_c \rangle$ (°K)	H_{c2} (kG)	$\gamma \times 10^{-3}$ erg/cm³ °K²	κ_l	κ_l/κ_0	H_c (kG)	H_{c1} (G)	H_p (kG)
NbC	9	16.9	2.3	13	24	0.80	120	130
40% NbC–60% TaC	11.8	14.1	1.2	8.1	30	0.99	190	214
TaC	10.2	4.6	1.1	3.2	16	0.81	220	185
$Mo_{56}C_{44}$	13	98.5	1.9	42	97	1.3	87	238
Mo_3Al_2C	10	156	5.0	53	35	1.7	91	181

$=\frac{1}{2}(H_s+H_n)$. We have ignored the possibility of a critical field H_{c3} due to a superconducting surface sheath[15] because all evidence to date indicates that the critical current versus the magnetic field plot drops sharply[4,16] in the vicinity of H_{c2} for the current densities used in this experiment. Also, surface irregularities of our samples and the geometry of our experiment would seem to minimize effects from the superconducting surface sheath.

The Ginzburg-Landau parameter $\kappa \approx \kappa_l$ (κ_0 is neglected with respect to κ_l) can be calculated from Eq. (3) and H_c is then obtained from Eq. (4). These values are also given in Table II.

Approximate values of the lower critical field H_{c1} derived from the relation[13]

$$H_{c1}=\frac{1}{\sqrt{2}}\frac{H_c}{\kappa}[\ln\kappa+0.08]\approx\frac{1}{\sqrt{2}}\frac{H_c}{\kappa_l}[\ln\kappa_l+0.08] \quad (6)$$

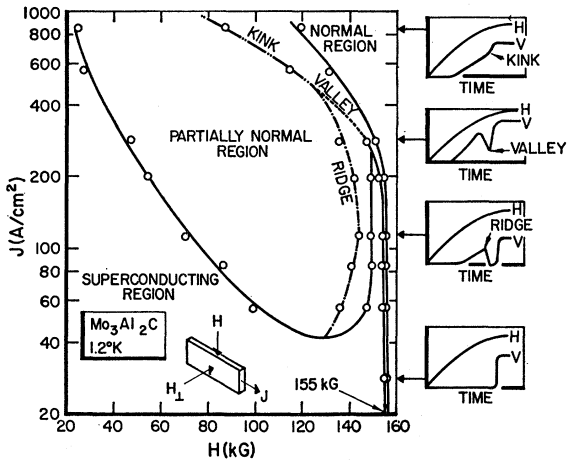

FIG. 6. The current densities are shown as a function of magnetic field between the superconducting region and the region which is partially normal, and between the partially normal region and the normal region for Mo_3Al_2C. The inserts on the right show schematically the observed pulsed magnetic field and the voltage across the potential leads on the sample as a function of time for four different current densities. The applied magnetic field was perpendicular to the current flow and the temperature was 1.2°K.

[15] D. Saint-James and P. G. de Gennes, Phys. Letters **7**, 306 (1963).

[16] W. DeSorbo, Phys. Rev. **135**, A1190 (1964).

are recorded in Table II. Also shown are the upper limits H_p to which superconductivity could possibly exist in a magnetic field according to the Clogston criterion.[17,18] It would appear that only the upper transition field of Mo_3Al_2C could possibly be affected by the Clogston limit. We believe that the physical parameters shown in Table II are fair estimates because $H_{c2}<H_p$ for all materials.

The consistency of the above assumption $\kappa_0 \ll \kappa_l$ is estimated from

$$\kappa_0=1.61\times10^{24}(T_c\gamma^{3/2}/N^{4/3})(S_f/S)^2, \quad (7)$$

where the average number of valence electrons per unit volume is N. For $Mo_{56}C_{44}$, $Mo_{60}C_{40}+2\%$ VC, and Mo_3Al_2C, N is assumed to be similar to all other carbides, namely 2.5×10^{23} cm^{-3} (their density is unknown). The ratio S/S_f of the free area of the Fermi surface to that of a free-electron gas is difficult to estimate but is assumed equal to $\frac{1}{2}$. This ratio is close to that of pure Nb for which one obtains a value[19] of 0.6. In Table II values of κ_l/κ_0 are shown which are considerably greater than unity for those materials listed. The only purpose of the very approximate estimate of the ratio κ_l/κ_0 is to show that for the materials recorded in Table II the coherence length is indeed limited by the electron mean free path and that it was justified to neglect κ_0 with respect to κ_l in deriving Eq. (5). For MoC and $Mo_{60}C_{40}+2\%$ VC, κ_l was not appreciably larger than κ_0 so estimates of γ, H_c, κ, and H_{c1} are not included.

ACKNOWLEDGMENTS

The authors are indebted to T. G. Berlincourt for many helpful discussions and the use of the pulsed field equipment, to R. R. Hake, L. Brewer, J. Garland, and M. Cohen for valuable discussions, and to P. F. Mac Doran, L. E. Valby, M. Pickus, J. Olson, and M. Wells for their experimental assistance.

[17] A. M. Clogston, Phys. Rev. Letters **9**, 266 (1962).

[18] B. S. Chandrasekhar, Appl. Phys. Letters **1**, 7 (1962).

[19] T. F. Stromberg and C. A. Swenson, Phys. Rev. Letters **9**, 370 (1962). These authors find for niobium, $S/S_f=0.18$, but T. G. Berlincourt and R. R. Hake (Ref. 4) have found a computational error. The correct value is 0.6.